Self-Induced Chaos in a Single-Mode Inversionless Laser

Sebastian Wieczorek and Weng W. Chow
Sandia National Laboratories, Albuquerque, New Mexico 87185-1086, USA
(Received 4 April 2006; published 14 September 2006)

A single-mode inversionless laser with a three-level phaseonium as an active medium can by itself exhibit complex nonlinear dynamics. Nonlinear interaction between two spectrally separated gain regions of the phaseonium and a lasing field gives rise to instabilities and chaotic self-pulsations of a type not observed in conventional lasers with population-inverted gain media. We calculate the bifurcation diagram and uncover multistability and a torus-doubling cascade in transition to chaos.

DOI: 10.1103/PhysRevLett.97.113903 PACS numbers: 42.60.Mi, 05.45.−a, 42.50.Gy, 42.55.−f

Nonlinear dynamics of lasers has been intensively studied since the laser invention in 1960. These studies provided invaluable insight into the nonlinear light-matter interaction in a cavity and uncovered phenomena including chaos, competition, excitability, and synchronization, found across different fields of science and engineering [1,2]. In particular, chaotic laser behavior motivated new technological applications such as secure chaotic communication and chaotic radars. Until 1989, the general belief was that lasers require population inversion.

During the last two decades, much attention has been devoted to the effects of atomic coherence and interference in a coherently prepared multilevel medium called phaseonium [3]. For the example from Fig. 1, it was found that phase coherence, or quantum coherence, created between two levels with a dipole-forbidden transition ($b \leftrightarrow c$) may cause unusual optical properties of the dipole-allowed transitions ($a \leftrightarrow b$) such as ultrahigh refractive index, vanishing absorption, and gain without population inversion. These discoveries led to phaseonium based lasers, called phasers [3], that do not require population inversion [4–8]. Owing to the nature of the active medium, phasers have nonlinearities that are very different from those found in conventional (population-inverted) lasers, and the resulting instabilities are not well understood. A further understanding of the phasers' nonlinear behavior, in particular, their differences from conventional lasers, is important from a fundamental viewpoint. The stability of various types of phaser output including continuous wave (cw), periodic, quasiperiodic, and chaotic lasing without inversion (LWI), as well as the possibility to control them, is becoming of great practical interest.

A single-mode three-level phaser is a paradigm of LWI [9] and the first step in understanding nonlinear dynamics of more complicated multimode phasers [10]. Although phasers show more potential for richer dynamics than conventional lasers, nonlinear dynamics analyses of LWI in single-mode, three-level phasers revealed only bistability and periodic self-pulsations [11–13]. These behaviors are much simpler than the Lorentz-type chaos reported in single-mode two- and three-level conventional lasers [1,14,15]. In particular, no chaotic LWI has yet been reported in single-mode, three-level phasers.

This Letter shows theoretically that a single-mode, three-level phaser can exhibit further instabilities and chaos of the type different than reported to date with lasers and phasers. We calculated the bifurcation diagram of a single-mode, three-level phaser and uncovered special codimension-two [16] bifurcation points that are sources of periodic, quasiperiodic, and chaotic LWI, as well as multistability. Most interesting is the self-induced torus-doubling cascade to chaotic LWI, a novel dynamical phenomenon which is not yet fully understood. It has been observed in numerical studies of dissipative media, coupled electronic circuits, forced climate model, and Navier-Stokes flow, as well as in experiments involving electrochemical reactions, arrays of convective oscillators, and ferroelectric crystals near phase transition [17]. A phaser is the first reported example of an optical system that shows a self-induced torus-doubling cascade and may contribute to a better understanding of this general phenomenon.

The results are obtained from solving the Maxwell-Bloch equations in the rotating wave approximation for a single-mode, three-level, ring-cavity phaser with the cavity resonant frequency ν_{cav} and decay rate γ_{cav}:

$$\dot{\Omega}_l = -\frac{\gamma_{\mathrm{cav}}}{2}\Omega_l - g\mathrm{Im}(\sigma_{ab}), \tag{1}$$

$$\dot{\rho}_{aa} = R_a - \frac{i}{2}[\Omega_l(\sigma_{ab} - \sigma_{ab}^*) + \Omega_p(\sigma_{ac} - \sigma_{ac}^*)], \tag{2}$$

$$\dot{\rho}_{bb} = R_b + \frac{i}{2}\Omega_l(\sigma_{ab} - \sigma_{ab}^*), \tag{3}$$

$$\dot{\sigma}_{ab} = -(\gamma_1 + i\Delta_l)\sigma_{ab} - \frac{i}{2}[\Omega_l(\rho_{aa} - \rho_{bb}) - \Omega_p\sigma_{cb}], \tag{4}$$

$$\dot{\sigma}_{ac} = -(\gamma_2 + i\Delta_p)\sigma_{ac} - \frac{i}{2}[\Omega_p(\rho_{aa} - \rho_{cc}) - \Omega_l\sigma_{cb}^*], \tag{5}$$

$$\dot{\sigma}_{cb} = -[\gamma_3 + i(\Delta_l - \Delta_p)]\sigma_{cb} - \frac{i}{2}(\Omega_l\sigma_{ac}^* - \Omega_p\sigma_{ab}). \tag{6}$$

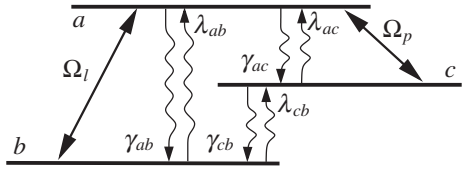

FIG. 1. A three-level scheme for inversionless gain.

The Rabi frequencies are defined as $\Omega_l(t) = \mu_{ab}E_l(t)/\hbar$ and $\Omega_p = \mu_{ac}E_p/\hbar$, where the slowly varying $E_l(t)$ and constant E_p are the real amplitudes of the lasing and coherent-pump electric fields, respectively, and μ_{ab} and μ_{ac} are the dipole moments. The gain coefficient is defined as $g = N|\mu_{ab}|^2\nu_l\Gamma/(\hbar\epsilon)$, where N is the atomic density, ν_l is the lasing-field frequency, and Γ is the optical-mode confinement factor. We assumed a time-independent pump-field phase, and the time derivative of the slowly varying lasing-field phase $\dot{\phi}_l = -g\mathrm{Re}(\sigma_{ab})/\Omega_l$ enters into $\Delta_l = \Delta_{\mathrm{cav}} - \dot{\phi}_l$, where the cavity detuning is defined as $\Delta_{\mathrm{cav}} = \nu_{ab} - \nu_{\mathrm{cav}}$. $\Delta_p = \nu_{ac} - \nu_p$, where ν_{ij} is the atomic frequency of the $i \leftrightarrow j$ transition and ν_p is the coherent-pump-field frequency. ρ_{ii} is the population of level i, and we assumed $\rho_{aa} + \rho_{bb} + \rho_{cc} = 1$. $R_a = -(\gamma_{ab} + \gamma_{ac} + \lambda_{ac})\rho_{aa} + (\lambda_{ab} - \lambda_{ac})\rho_{bb} + \lambda_{ac}$ and $R_b = (\gamma_{ab} - \gamma_{cb})\rho_{aa} - (\gamma_{cb} + \lambda_{ab} + \lambda_{cb})\rho_{bb} + \gamma_{cb}$ describe incoherent pump and decay processes, where γ_{ij} is the decay rate from i to j, and λ_{ij} is the pump rate from j to i, as indicated in Fig. 1. σ_{ij} are the slowly varying complex amplitudes of the off-diagonal elements of density matrix $\{\rho_{ij}\}$, and $\gamma_1 = (\gamma_{ab} + \gamma_{ac} + \lambda_{ab} + \lambda_{cb})/2$, $\gamma_2 = (\gamma_{ab} + \gamma_{ac} + \gamma_{cb} + \lambda_{ac})/2$, and $\gamma_3 = (\gamma_{cb} + \lambda_{ab} + \lambda_{ac} + \lambda_{cb})/2$ are the corresponding dephasing rates [12].

The stable fixed point of Eqs. (1)–(6) with $\Omega_l = 0$ corresponds to a phaser below threshold (off), and a stable fixed point with $\Omega_l > 0$ corresponds to cw LWI. Periodic orbit corresponds to LWI with periodically self-pulsating intensity (sp). As the parameters are changed, the solutions of Eqs. (1)–(6) can change as well. Qualitative changes in the system's dynamics, i.e., the bifurcations [16], are calculated with the bifurcation continuation package AUTO [18]. Transition from below threshold to cw LWI occurs typically via supercritical pitchfork bifurcation. In supercritical Hopf bifurcation, the stable point becomes unstable by giving rise to stable periodic orbit. In subcritical Hopf bifurcation, the unstable point may become stable by giving rise to unstable periodic orbit. A pair of stable and unstable periodic orbits may disappear in the saddle node of limit cycle bifurcation.

Bifurcations of Eqs. (1)–(6) are calculated in the $(\Omega_p, \Delta_{\mathrm{cav}})$ plane for $\Delta_p = 0$, $\gamma_{\mathrm{cav}} = 0.03\gamma$, $\gamma_{ab} = 0.055\gamma$, $\gamma_{ac} = 0$, $\gamma_{cb} = 0.0055\gamma$, $\lambda_{ab} = 0.045\gamma$, $\lambda_{ac} = 0.45\gamma$, and $\lambda_{cb} = 0$. In the absence of the lasing and coherent-pump field we have $\rho^0_{aa} = 0.45$, $\rho^0_{bb} = 0.55$, and $\rho^0_{cc} = 0$. Parameters are scaled with respect to a free parameter γ, and g is given in the figure captions. Chaos is found for $g/\gamma^2 = 100$. Choosing $\gamma = 4 \times 10^8$ s^{-1}, using the definition of g and assuming 1 D for μ_{ij}, 10 μm laser wavelength, and $\Gamma = 10^{-4}$, the required atomic density for observing chaos is $N = 4.5 \times 10^{23}$ m^{-3}. For room temperature, this corresponds to an active medium gas pressure of 1842 Pa or 13.9 Torr. The dephasing rates, $\gamma_i \sim 10^8$ s^{-1}, and the population decay rates, $\gamma_{ij} \sim 10^6$ s^{-1}, are consistent with the values found in molecular gases. Furthermore, $\Omega/\gamma = 1$ means a drive field intensity of 21 W/cm^2, and $\gamma_{\mathrm{cav}} = 1.2 \times 10^7$ s^{-1}.

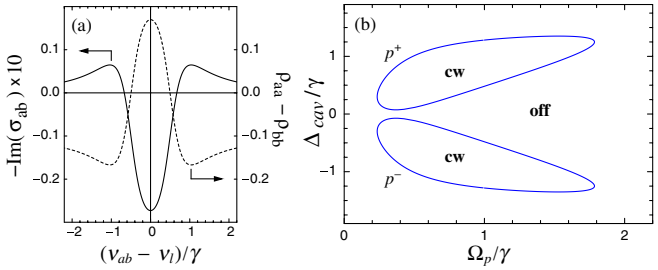

FIG. 2 (color online). (a) Gain (solid curve) and population difference (dashed curve) for the three-level phaseonium from Fig. 1 without a cavity; calculated with Eqs. (2)–(6) for $\Omega_l/\gamma = 0.5$ and $\Omega_p/\gamma = 1$. (b) Bifurcation diagram of LWI for the three-level phaseonium inside a ring-cavity; calculated with Eqs. (1)–(6) for $g/\gamma^2 = 1$. Regions of LWI are bounded by the p curves; cw marks continuous wave LWI and off is for laser below threshold. The laser is operated near its lasing threshold.

The phaseonium gain per unit length for the $a \leftrightarrow b$ transition is related to the slowly varying polarization σ_{ab} according to gain $= -g\sqrt{\epsilon_r}\mathrm{Im}(\sigma_{ab})/(c\Gamma\Omega_l)$. Figure 2(a) shows the gain profile (solid curve) and population inversion (dashed curve) assuming no cavity and a weak cw probe Ω_l. For incoherent pump and decay rates such that $\rho^0_{cc} - \rho^0_{aa} < 0$, quantum coherence σ_{cb} induces two spectrally separated inversionless-gain regions [9,12]. An interesting question arises as to what happens when this phaseonium is placed inside a cavity.

Figure 2(b) depicts the bifurcation diagram in the $(\Delta_{\mathrm{cav}}, \Omega_p)$ plane in the close vicinity of the lasing threshold. The cw LWI occurs detuned from the atomic resonance inside two islands bounded by the pitchfork bifurcation curves p^+ and p^-. The diagram from Fig. 2(b) may change drastically if the laser is operated further above threshold. In particular, as g increases, the two LWI regions from Fig. 2(b) grow in size and interact in a very nonlinear fashion. The previous studies focused on lasing near threshold. They reported bistability and periodic self-pulsations around zero cavity detuning where the two LWI regions overlap slightly [11–13]. This Letter uncovers further and more complicated LWI instabilities characteristic for inversionless lasing far above threshold.

Figure 3 shows the bifurcation diagrams in the $(\Delta_{\mathrm{cav}}, \Omega_p)$ plane that are typical for LWI far above threshold. The two LWI regions overlap significantly, and for $g/\gamma^2 \gtrsim 7$, there are four intersection points between p^+

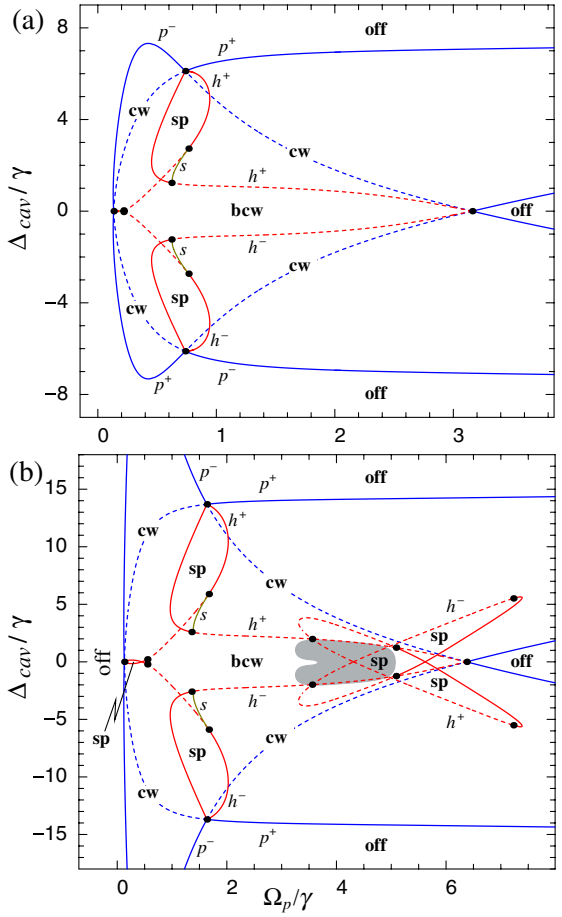

FIG. 3 (color online). Bifurcation diagram of LWI for (a) $g/\gamma^2 = 25$ and (b) $g/\gamma^2 = 100$. Region of LWI is bounded by the solid parts of the p curves; cw marks continuous wave LWI, bcw marks bistable continuous wave LWI, unshaded sp marks periodic self-pulsing LWI, shaded sp roughly marks nonperiodic self-pulsing LWI, and off is for laser below threshold. The laser is operated far above its lasing threshold.

and p^-, called codimension-two double-pitchfork bifurcations. At each point, (i) p^+ and p^- change from supercritical (solid curves) to subcritical (dashed curves) and (ii) Hopf bifurcation curves h appear, giving rise to regions of periodic self-pulsations (solid parts of h) and bistable cw LWI (dashed parts of h). Also, there are saddle node of limit cycle bifurcations s which partially bound regions of periodic self-pulsations. In contrast to Fig. 2(b), the diagram in Fig. 3(a) has a region of bistability at the atomic resonance and three regions of periodic self-pulsations: two located off the atomic resonance and a significantly smaller one at the origin of the $(\Delta_{\mathrm{cav}}, \Omega_p)$ plane [more distinct in Fig. 3(b)].

Upon further increasing g, two additional Hopf bifurcation curves h^+ and h^- appear, giving rise to additional regions of self-pulsations [Fig. 3(b)]. Most importantly, there are now four intersection points between different $h^{+(-)}$ curves, called codimension-two double-Hopf bifurcations. Out of 11 possible cases of a double-Hopf bifurcation [16] we encountered the most complicated one, which involves quasiperiodic and chaotic self-pulsations indicated roughly by the shaded region in Fig. 3(b). Here, we present two highlights of complicated LWI: torus doubling to chaos and multistability.

The torus-doubling cascade shows some similarities to the well-known infinite period-doubling cascade [19] but differs in at least two significant aspects. First, torus doubling requires at least a four-dimensional vector field. Second, a torus-doubling cascade involves an interplay between two types of transition to chaos, namely, period doubling and the breakup of tori. In fact, the tori break up within certain parameter intervals around each doubling point. These intervals eventually overlap, owing to the accumulation of subsequent doubling points, and this effect truncates the doubling cascade. If the two frequencies of the torus f_1 and f_2 are comparable, one expects long intervals with broken-up tori and only a few doubling steps. If $f_1 \gg f_2$, as is in our case, one expects short intervals with broken-up tori (possibly below what can be detected numerically) and many more torus-doubling steps [20]. In Fig. 4, the torus-doubling cascade is illustrated with (top row) attractors in the Poincaré section and (bottom row) corresponding power spectra of the phaser field

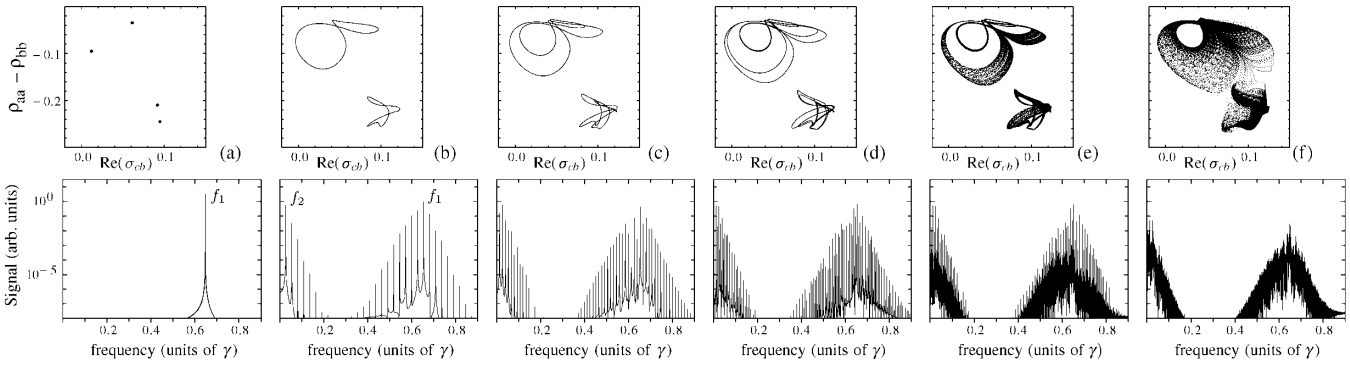

FIG. 4. Torus doubling in transition to chaotic LWI shown as (top row) attractors in the projection of the Poincaré section $\{\mathrm{Im}(\sigma_{ab}) = 0\}$ and (bottom row) power spectra of $\Omega_l(t)^2$. $g/\gamma^2 = 100$, $\Omega_p/\gamma = 4.4$, and from (a) to (f) $\Delta_{\mathrm{cav}}/\gamma = 1.0$, 0.3, 0.2, 0.14, 0.13, and 0.1.

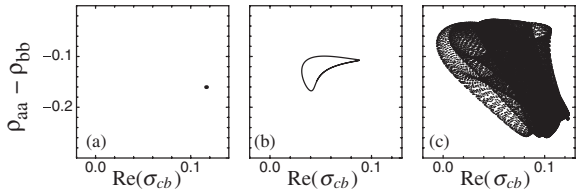

FIG. 5. Multistability between (a) stationary point, (b) periodic orbit, and (c) doubled torus for $g/\gamma^2 = 100$, $\Omega_p/\gamma = 4.4$, and $\Delta_{\text{cav}}/\gamma = 0.2$.

intensity. Figure 4(a) shows periodic orbit of frequency f_1, born in the saddle node of limit cycle bifurcation inside the shaded region in Fig. 3(b). This orbit crosses the Poincaré section 4 times. With decreasing Δ_{cav}, this periodic orbit becomes unstable via torus bifurcation and gives rise to a stable torus shown in the Poincaré section as two invariant circles [Fig. 4(b)]. Motion on the two-dimensional torus from Fig. 4(b) represents self-pulsating LWI with two frequencies, f_1 and f_2. The trajectory appears to completely fill the two circles in the Poincaré section indicating that these two frequencies are incommensurate, and the phaser output is quasiperiodic. The power spectrum has peaks at all integer linear combinations of f_1 and f_2. In torus doubling, a two-dimensional torus becomes unstable and a stable doubled torus appears [Fig. 4(c)]. This is accompanied by the appearance of additional peaks in the spectrum which can be expressed by integer linear combinations of $f_1/2$ and $f_2/2$. We were able to distinguish four consecutive torus doublings before chaotic attractor emerged with a spectrum that is a mixture of a continuous background and strong discrete peaks [Fig. 4(e)]. With further decrease in Δ_{cav}, we observed a transition to full-blown chaos with hardly any discrete peaks in the spectrum [Fig. 4(f)]. Another interesting phenomenon found inside the shaded region of Fig. 3(b) is multistability. An example involving fixed point, periodic orbit, and the doubled torus from Fig. 4(c) is shown in Fig. 5. The torus-doubling cascade can be reached by following the stable stationary point until it destabilizes along the dashed part of h^-.

In conclusion, this Letter investigates self-induced nonlinear behavior of a single-mode, three-level phaser. We considered conditions under which quantum coherence induces inversionless gain at two spectrally separated regions off the atomic resonance. Such a gain profile gives rise to two inversionless-lasing solutions. In the vicinity of the lasing threshold, each of the two solutions exist inside a separate region of inversionless lasing in the plane of the coherent-pump strength and cavity detuning. However, as the laser operates further above threshold, the two regions of inversionless-lasing overlap, giving rise to strong optical nonlinearities. These nonlinearities, governed by the processes of self- and cross saturation between the two lasing solutions [12], lead to special codimension-two double-pitchfork and double-Hopf bifurcations in the bifurcation diagram. The more interesting double-Hopf bifurcations are sources of multistability and complicated inversionless self-pulsations of the type distinctively different from instabilities found in conventional lasers. In particular, we uncovered the torus-doubling cascade in transition to chaotic lasing without inversion. A phaser is the first reported example of an optical system that shows this interesting bifurcation scenario. Note that single-mode conventional lasers have a single spectral gain region, single lasing solution, and cannot exhibit instabilities arising from the nonlinear interaction between different lasing solutions induced by quantum coherence.

This work is supported in part by the U.S. Department of Energy under Contract No. DE-AC04-94AL8500 and the Alexander von Humboldt Foundation.

[1] C. O. Weiss and R. Vilaseca, *Dynamics of Lasers* (VCH Verlagsgesellschaft, Weinheim, Germany, 1991).
[2] *Fundamental Issues of Nonlinear Laser Dynamics: Concepts, Mathematics, Physics, and Applications International Spring School*, edited by B. Krauskopf and D. Lenstra, AIP Conf. Proc. No. 548 (AIP, New York, 2000).
[3] M. O. Scully, Phys. Rep. **219**, 191 (1992).
[4] S. E. Harris, Phys. Rev. Lett. **62**, 1033 (1989).
[5] M. O. Scully, S. Y. Zhu, and A. Gavrielides, Phys. Rev. Lett. **62**, 2813 (1989).
[6] O. Kocharovskaya, Phys. Rep. **219**, 175 (1992).
[7] J. Mompart and R. Corbalán, J. Opt. B **2**, R7 (2000).
[8] A. S. Zibrov *et al.*, Phys. Rev. Lett. **75**, 1499 (1995).
[9] P. Mandel and O. Kocharovskaya, Phys. Rev. A **46**, 2700 (1992).
[10] Y. V. Radeonychev *et al.*, J. Opt. B **1**, 580 (1999).
[11] V. J. Sánchez-Morcillo, E. Roldán, and G. J. de Valcárel, Quantum Semiclass. Opt. **7**, 889 (1995).
[12] A. G. Vladimirov *et al.*, Phys. Rev. E **57**, 1499 (1998).
[13] J. Mompart, C. Peters, and R. Corbalán, Phys. Rev. A **57**, 2163 (1998).
[14] H. Haken, Phys. Lett. **53A**, 77 (1975).
[15] J. V. Moloney, J. S. Uppal, and R. G. Harrison, Phys. Rev. Lett. **59**, 2868 (1987).
[16] Yu. A. Kuznetsov, *Elements of Applied Bifurcation Theory* (Springer, New York 1995).
[17] H. W. Broer, C. Simó, and R. Vitolo, Nonlinearity **15**, 1205 (2002); J. I. Kim, H. K. Park, and H. T. Moon, Phys. Rev. E **55**, 3948 (1997); L. van Veen, Physica (Amsterdam) **210D**, 249 (2005); J. M. Flesselles, V. Croquette, and S. Jucquois, Phys. Rev. Lett. **72**, 2871 (1994); J. C. Shin and S. I. Kwun, Phys. Rev. Lett. **82**, 1851 (1999).
[18] E. Doedel *et al.*, computer code AUTO, http://sourceforge.net/projects/auto2000.
[19] A. Arnéodo, P. H. Coullet, and E. A. Spiegel, Phys. Lett. **94A**, 1 (1983).
[20] F. Schidler, H. M. Osinga, and W. Vogt, SIAM J. Appl. Dyn. Syst. **4**, 459 (2005).